ELASTOHYDRODYNAMICS OF TENSIONED WEB ROLL COATING PROCESS

Márcio da S. Carvalho
Department of Mechanical Engineering, Pontifícia Universidade Católica do Rio de Janeiro.
Rua Marquês de São Vicente, 225, Gávea. Rio de Janeiro, RJ, 22453-900, Brazil.
Email: msc@mec.puc-rio.br

Abstract

Coating process is an important step in the manufacturing of different products, such as paper, adhesive and magnetic tapes, and photographic films. The tensioned web roll coating is one the several methods used by different industries. It relies on the elastohydrodynamic action between the fluid and the deformable substrate for transferring and applying the liquid. The main advantage of this method is its ability to apply very thin liquid layers at relative small cost. This work analyzes this elastohydrodynamic action by solving the differential equations that govern the liquid flow and the web deformation. The goal is to determine the operating conditions at which the process is two-dimensional and defect free. The equations are discretized by the Galerkin / finite element method. The resulting non-linear system of equations is solved by Newton's method coupled with pseudo-arc-length continuation in order to be able to obtain solutions around turning points.

Key words: elastohydrodynamics, finite element method, coating process, tensioned web.

1. INTRODUCTION

In industrial coating processes, one or several liquid layers are deposited on a substrate and are then dried to form a solid film that serves a specific function. This process is vital in the manufacturing of different products, like paper, adhesive and magnetic tapes, magnetic disks, photographic films, and many others. The different ways of depositing a liquid on the substrate lead to different coating methods. Some of these methods rely on the interaction between hydrodynamic forces exerted by the flowing coating liquid and forces exerted by a deformable solid boundary that confines the flow, i.e. an elastohydrodynamic interaction. The main advantage of elastohydrodynamic coating system is their ability to apply very thin liquid layers with less sensitivity to mechanical tolerances at a relative small cost, when compared to more sophisticated pre-metered coating method, such as slot, slide and curtain coating (Pranckh and Coyle, 1997).

Of the many examples of elastohydrodynamic coating systems, the tensioned web roll coating uses only the deformable substrate without any external mechanical support to provide the elastic boundary for the liquid flow and to impose load in the coating bead. In tensioned web roll coating, the liquid is transferred to the substrate as it passes over a rotating roll, as illustrated in Fig.1. The roll and the substrate can be moving in the same direction, i.e. forward mode, or in opposite directions, called a reverse mode. The film thickness deposited

on the web is a function of the roll and web speeds, liquid viscosity, substrate stiffness and tension, and the wrapping angle of the substrate over the rotating roll. It is important to understand this elastohydrodynamic action in order to be able to predict and optimize this important industrial process.

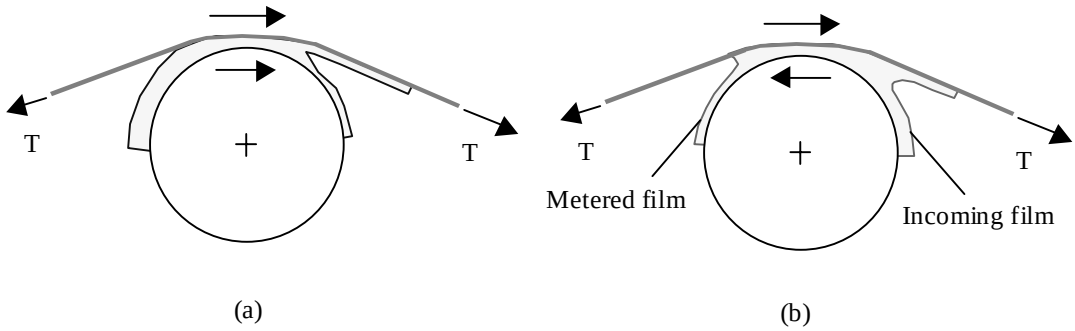

Figure 1: Tensioned web roll coating: (a) forward mode; (b) reverse mode.

This work analyzes the flow in a tensioned web roll coating bead operating in the reverse mode, as shown in Fig.1(b). The liquid is brought to the bead as a layer in the applicator roll, referred as the incoming layer. It is supplied to the roll by dip coating or by a slot die located upstream the coating bead. Part of the liquid is transferred to the substrate and the remaining stays on the roll creating what is usually called the metered film. The goal of this work is to determine the metered film thickness as a function of the operating parameters and the operating conditions at which the process is two-dimensional and defect free.

The differential equations that govern the liquid flow and the substrate deformation are discretized by the Galerkin / finite element method. The resulting non-linear system of equations is solved by Newton's method coupled with pseudo-arc-length continuation in order to be able to obtain solutions around turning points. The theoretical results are used to construct an operating window for the process that is in agreement with some experimental data available.

2. ELASTOHYDRODYNAMIC MODEL

2.1. Governing Equations

The configuration of the problem analyzed in this work is illustrated in Fig.2. The roll that brings the liquid into the transfer region is moving from right to left in the figure. The substrate is moving in the opposite direction and takes part of the liquid with it. The remaining liquid stays in the roll and is later removed from it by a scraper, not analyzed here. The liquid traction deforms the tensioned substrate. The flow and the deformation are coupled in what is called elastohydrodynamic behavior. This type of problem was first analyzed by Eshel and Elrod (1965, 1967).

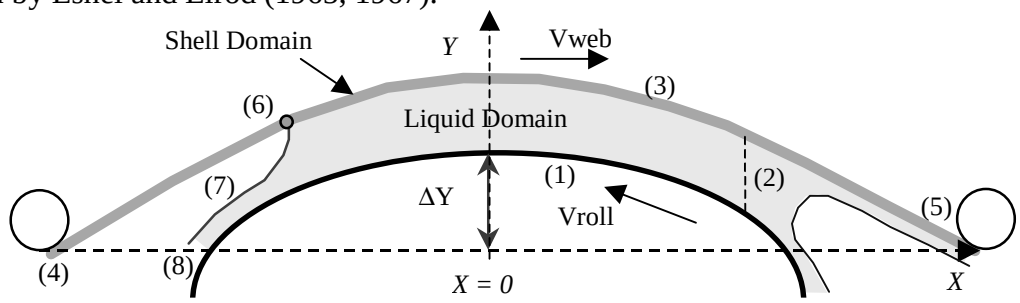

Figure 2: Sketch of domain of calculation. Ω_f is the fluid domain and Ω_s is the shell domain.

It is important to characterize the position of the moving roll relative to the upstream and downstream idlers that guide the moving web. The relative position can be characterized by the distance ΔY from the top of the roll to the axis that passes through the idlers, called here the x-axis. The coordinate x = 0 is defined in the middle of the line that connects the two idlers, as indicated in the figure. When $\Delta Y<0$, the web does not touch the roll. When $\Delta Y>0$, the web wraps around a portion of the roll.

The web is assumed to be infinitely wide, and therefore the flow in the transverse direction is neglected. The motion of the liquid is described by the Navier-Stokes equation and continuity equation for incompressible Newtonian fluid:

$$\rho \mathbf{v}\cdot\nabla\mathbf{v} - \nabla\cdot\left[-p\mathbf{I} + \mu\left(\nabla\mathbf{v} + (\nabla\mathbf{v})^T\right)\right] = 0 \quad \text{and} \quad \nabla\cdot\mathbf{v} = 0 \tag{1}$$

together with appropriate boundary conditions. ρ and μ are the liquid density and viscosity, respectively. The deformation of the web is modeled by the equations of cylindrical shells:

$$\begin{aligned} &\frac{dT}{d\xi} + \kappa\frac{d}{d\xi}(\kappa D) + P_t + W_t = 0 \\ &-\frac{d^2}{d\xi^2}(\kappa D) + \kappa T + P_n + W_n = 0 \\ &\frac{d^2x}{d\xi^2} + \kappa\frac{dy}{d\xi} = 0 \quad \text{or} \quad \frac{d^2y}{d\xi^2} - \kappa\frac{dx}{d\xi} = 0. \end{aligned} \tag{2}$$

ξ is the coordinate along the web. T and κ are the web tension and curvature at each position, and x and y are the Cartesian coordinates of points on the web. The web stiffness $D \equiv Et^3/12(1-\upsilon^2)$ is a function of the Elastic Modulus E, Poisson ratio υ, and thickness of the web t. P_t and P_n are the forces on the web in the tangential and normal direction.

The goal of this work is to analyze the amount of liquid that remains on the roll, i.e. the metered film thickness, at different operating conditions. Because the flow between the roll and the substrate is almost rectilinear far from the free surfaces and this work is only interested in the behavior of the metered film, the free surface in the upstream side of the coating gap is removed from the problem for simplicity. In the analysis presented here, it is substituted by what is called a flooded inlet, i.e. an artificial boundary condition used to reduce the side of the domain of calculation, which is shown in Fig.2. The domain is divided into two different subdomains: One where the Navier-Stokes equation is solved (Ω_f), and the other where the cylindrical shell equations are solved (Ω_s). At the roll surface, labeled (1) in Fig.2, the no-slip and no-penetration conditions apply. The artificial inlet boundary (2) was located far enough that its location had no effect on the predictions reported here. On that position, the liquid pressure is assumed to be constant (atmospheric). At the interface between the liquid and the flexible substrate (3), the liquid velocity is equal to the web velocity, and the loading force responsible for the web deformation is the traction exerted by the liquid. In one extreme of the substrate (4), the position, curvature and web tension have to be specified; in the other (5), only the position and curvature are specified. The point where the liquid first wets the substrate (6) is called the dynamic contact line. There, a local Navier-slip condition has to be used, otherwise a stress singularity would appear. At the free surface (7), the kinematic condition and a force balance in the form of the Young-Laplace equation, that takes into account the effect of surface tension, are imposed. At the artificial outlet place, the liquid traction is assumed to vanish.

This situation is governed by the following dimensionless groups:

Reynolds number : $\mathrm{Re} \equiv \dfrac{\rho V R}{\mu}$;

Capillary number: $\mathrm{Ca} \equiv \dfrac{\mu V}{\sigma}$;

Speed ratio: $S \equiv \dfrac{V_{web}}{V_{roll}}$;

Tension number : $\tau \equiv \dfrac{\mu V}{T}$;

Elasticity number : $N_{ES} \equiv \dfrac{D}{TR^2} = \dfrac{Et^3}{12(1-\upsilon^2)TR^2}$;

Wrapping position : $\alpha \equiv \dfrac{\Delta Y}{R}$.

2.2. Solution Method

The governing equations and the boundary conditions give rise to a free boundary problem. The location of the web and the free surface are unknown a priori. The basis of treating such problems is recounted briefly here. Fuller accounts were given by Kistler and Scriven (1983, 1984), Sackinger et al. (1996), and Carvalho and Scriven (1997).

In order to solve a free boundary problem using standard techniques for boundary value problems, the set of differential equations posed in the unknown physical domain has to be transformed to an equivalent set defined in a known, fixed reference domain. This approach has been extensively used to solve viscous flow with liquid / air interface. In that class of problem, the position of the interface is implicitly located by imposing the kinematic boundary condition at the free surface. In the situation studied here, the position of the web is implicitly located by imposing the system of ordinary differential equations (3). The transformation of the set of differential equations that governs the problem is made by a mapping $\mathbf{x} = \mathbf{x}(\boldsymbol{\xi})$ that connects the physical domain, parameterized by the position vector $\mathbf{x} = (x, y)$, and the reference domain, parameterized by $\boldsymbol{\xi} = (\xi, \eta)$. The inverse of the mapping is governed by a pair of elliptic differential equations identical with those encountered in the dilute regime of diffusional transport. The coordinate potentials ξ and η satisfy

$$\nabla \cdot (D_\xi \nabla \xi) = 0 \quad \text{and} \quad \nabla \cdot (D_\eta \nabla \eta) = 0 \tag{3}$$

The Navier-Stokes equation (1), the substrate deformation (2) and the mesh generation equations (3) together with the respective boundary conditions were solved by the Galerkin / finite element method. Biquadratic basis functions were used to represent both the velocity and the mapping from the reference to the physical domain. The basis functions used to represent the pressure field were piecewise, linear and discontinuous.

The resulting non-linear system of algebraic equations for the coefficients of the basis functions was solved by Newton's method. The domain was divided into 484 elements with 9144 unknowns. The computations were performed in a HP model J-200 workstation, and each solution took approximately 6 minutes to be computed.

In order to obtain solutions at large wrapping angles, i.e., large values of ΔY, a good initial guess is vital. The procedure adopted was to first obtain solutions with the roll far from the web, i.e., $\Delta Y < 0$. At these conditions, the pressure that builds up in the liquid is very small leading to small web deformation. A solution can be obtained even with a poor initial guess. After a solution is computed, a first-order, arc-length continuation on the position of

the roll was used to obtain solutions at the relevant set of parameters and to determine turning points on the solution path.

3. THEORETICAL PREDICTIONS

The domain configuration of a sequence of solutions at Ca = 0.1 and $\Delta Y / R = -10^{-3}$ (the web does not touch the roll) and rising speed ratio is shown in Fig.3. As the web speed increases, the dynamic contact line is pulled close and then through the plane of x = 0. This behavior occurs at all Capillary Numbers, as illustrated in Fig.4.

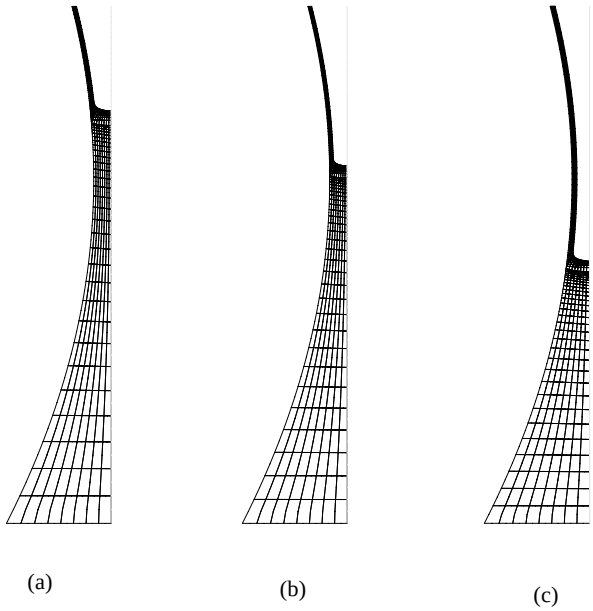

Figure 3: Flow states at Ca = 1, $\Delta Y / R = -10^{-3}$ and (a) S = 0.6; (b) S = 0.7; and (c) S = 0.8.

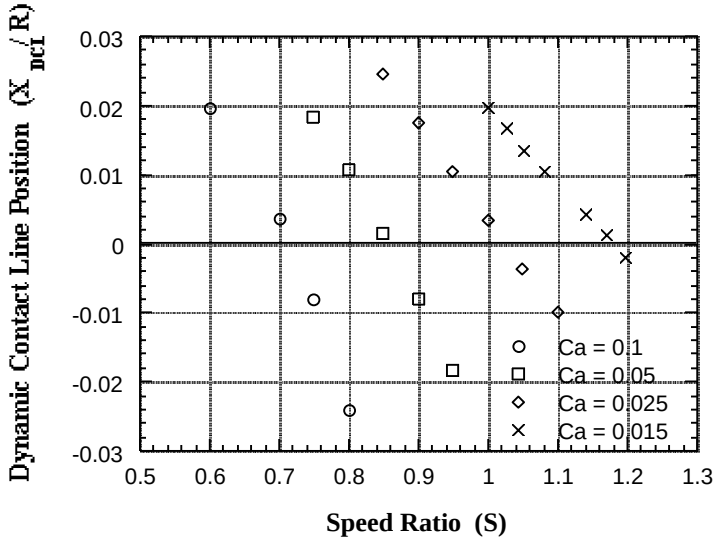

Figure 4: Dynamic contact line position as a function of speed ratio and Capillary number.

The metered film thickness at all the flow states shown in Fig.4 is plotted in Fig.5. First the film thickness decreases as the speed ratio is raised: As the web speed increases, the substrate carries more liquid with it and less liquid is left on the roll surface. However, above the speed ratio at which the dynamic contact line passes through the plane x = 0, the behavior

of the metered film changes completely. Its thickness increases with speed ratio. At each Capillary Number there is a minimum metered film thickness possible.

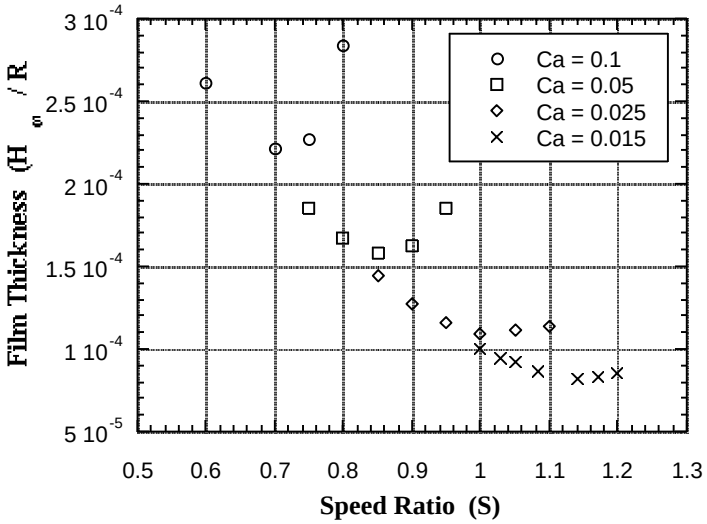

Figure 5: Film thickness of the metered film as a function of speed ratio and Capillary number.

When tensioned web is used to transfer a film to a substrate, it is desired to transfer all or most of the liquid deposited on the roll. Therefore, the metered film thickness has to approach zero. As it is clear from Fig.5, this can not be achieved with the configuration where the web is not wrapping part of the roll. The effect of pushing the roll against the substrate is examined in the following two figures. Figure 6 shows the free surface profile at Ca = 0.1 and S = 0.7 and different roll positions (*ΔY/R*). As the roll is pushed against the substrate, the meniscus moves away from the plane x = 0.

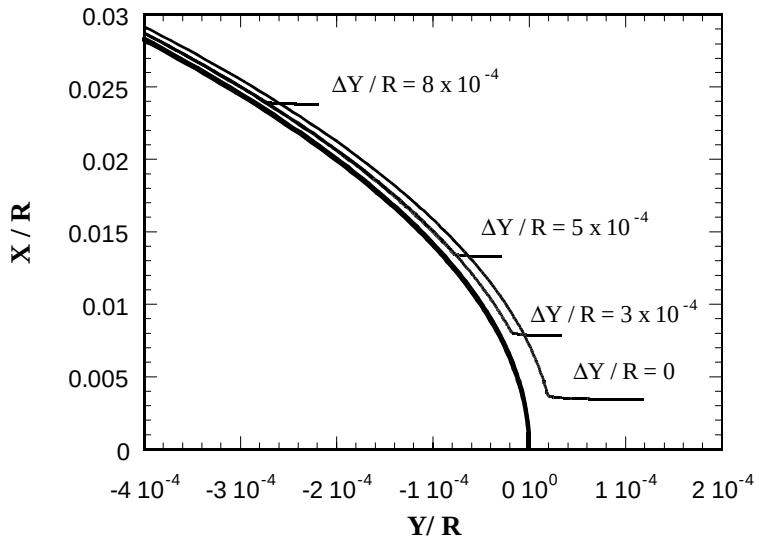

Figure 6: Free surface profile at Ca = 0.1 and S = 0.7 as a function of ΔY/R.

The film thickness at different wrapping angles and speed ratio is shown in Fig. 7. At small wrapping angles, i.e. $\Delta Y/R < 10^{-4}$, solutions could be obtained at all speed ratio, and there was a minimum thickness. It occurred at the speed ratio at which the dynamic contact line passed through the place x = 0, as discussed before. At large wrapping angles, a minimum film thickness was not observed, however there was always a speed ratio above which no two-dimensional, steady state solution could be obtained.

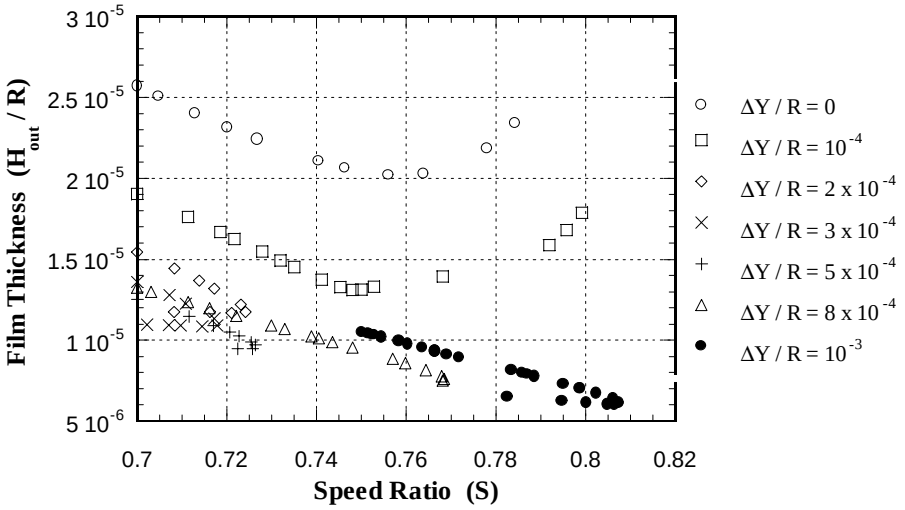

Figure 7: Film thickness of metered film as a function of speed ratio and wrapping angle.

The theoretical predictions are used to construct an operating window for this coating process, i.e. a diagram that shows the process condition as a function of wrapping angle and speed ratio, as shown in Fig.8. The speed ratio at which the turning point occurs is associated with the condition at which the metered film ceases to be continuous in the transverse direction (the flow is not two-dimensional) and breaks into stripes of liquid, generally called rivulets. The speed ratio at which the dynamic contact line passes through the plane x = 0 is associated with the onset of an unstable bead that leads to a coating defect known as seashore. In the figure, the clear region represents the area of stable and two-dimensional flow.

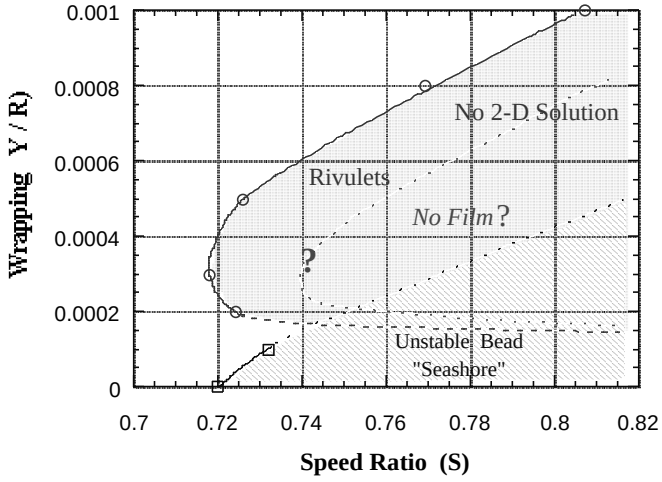

Figure 8: Coating window for the tensioned web roll coating process.

4. FINAL REMARKS

Tensioned web roll coating is used to produce very thin liquid layers at relative small cost. Another important advantage of this method is that the film thickness and quality is fairly insensitive to mechanical tolerances. This work presented a theoretical approach to determine the operating window of this process operating in a reverse mode. The equations

that describe the liquid motion and substrate deformation were solved by the Galerkin / finite element method.

The results show the speed ratio at which the metered film breaks into rivulets and the conditions at which the bead becomes unstable, leading to a coating defect known as seashore. These two limits of operation determined theoretically were validated with some experimental evidences. Figure 9 illustrates flow visualization of the coating bead looked from the back of a transparent applicator roll at two different speed ratio. At speed ratio S = 0.75, the metered film left on the roll is in the form of rivulets, as predicted by the theoretical model. Rising the speed ratio to even higher values, S = 1, in Fig.9(b), the coating bead becomes unstable, also as predicted by the model.

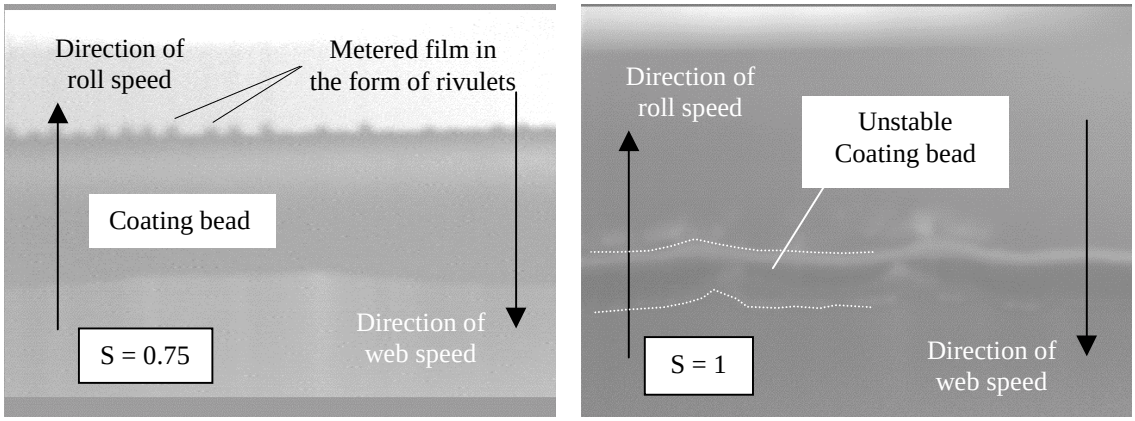

Figure 9: Flow visualization of metered film in the form of rivulets (S = 0.75) and unstable coating bead (S = 1).

5. REFERENCES

- Carvalho M. S. and Scriven L. E. 1997. "Flows in Forward Deformable Roll Coating Gaps: Comparison Between Spring and Plane Strain Model of Roll Cover". Journal of Computational Physics, vol.138(2), pp.449-479.
- Eshel A. and Elrod H.G. 1965. "The Theory of Infinitely Wide, Perfectly Flexible, Self-Acting Foil Bearing". Journal of Basic Engineering, vol. 87, pp. 831-836.
- Eshel A. and Elrod H.G. 1967. "Stiffness Effects on the Infinitely Wide Foil Bearing". Journal of Lubrication Technology, vol. 89}, pp.92-97.
- Kistler S.F. and Scriven L.E. 1983. "Coating Flows. Computational Analysis of Polymer Processing" (Eds. J.R.A. Pearson and S.M. Richardson). Applied Science Publishers, London, pp.243.
- Kistler S.F. and Scriven L.E. 1984. "Coating flow theory by finite element and asymptotic analysis of the Navier-Stokes system". International Journal for Numerical Methods in Fluids, vol. 4, pp.207.
- Pranckh F.R. and Coyle D.J. 1997. "Elastohydrodynamic Coating Systems", in Liquid Film Coating: Scientific Principles and their Technological Implications (ed. S.F. Kistler and P.M. Schweizer).
- Sakinger P.A., Schunk P.R. and Rao R.R. 1996. "A Newton-Raphson Pseudo-Solid Domain Mapping Technique for Free and Moving Boundary Problems: A Finite Element Implementation". Journal of Computational Physics, vol. 125, pp.83-103.